IMPACT OF CLIMATE VARIABILITY ON THE CIRCULATION OF AN EAST-AUSTRALIAN BAY

Ulf Gräwe[1], Joachim Ribbe[2], Jörg-Olaf Wolff[1]
[1]University of Oldenburg, Oldenburg, Germany, [2]University of Southern Queensland, Toowoomba, Australia

1. INTRODUCTION

In subtropical climates where evaporation is likely to exceed the supply of freshwater from precipitation and river run-off, large coastal bays, estuaries and near shore coastal environments are often characterized by inverse circulations and hypersalinity zones (Tomczak and Godfrey 2003, Largier et al. 1997). An inverse circulation is characterized by sub-surface flow of saline water away from a zone of hypersalinity towards the open ocean. This flow takes place beneath a layer of inflowing oceanic water and leads to salt injections into the ocean (Brink and Shearman 2006), examples for such seas include the European Mediterranean Sea, the Gulf of California, the Persian Gulf, the Red Sea and several Australian estuaries and coastal bays (Ribbe 2006, deCastro et al. 2004, Lavin et al. 1998).
Recently observed climate changes suggest a widening of the tropical climate belt over the last few decades that is likely to have a significant impact on subtropical climates (Seidel et al. 2008). It leads to shifts in atmospheric and oceanic circulation pattern that together determine the distribution of rainfall. In Australia, where climate is characterized by significant inter annual variability in rainfall (Murphy and Ribbe 2004), longer lasting trends in annual rainfall have been observed since about 1950 (Shi et al. 2008a). Along the densely populated east coast rainfall has declined by more than 200 mm (1951-2000). This reduction of about 20 % in total annual rainfall has caused persistent drought conditions in the last two decades. These shifts have been attributed to changes in large scale climate system processes such as the Southern Annular Mode, the Indian Ocean Dipole and the El Nino Southern Oscillation (Shi et al. 2008b). These changes that are linked to a widening of the tropical belt are projected to persist into the future. The adjustments are associated with an increased heat transport by the southward flowing East Australia Current (EAC) that has been attributed to atmospheric circulation changes (Cai et al. 2005). The changes in rainfall are accompanied by a rise in near surface atmospheric temperature that along the east coast of Australia is in the order of about 0.1 °C per decade (Beer et al. 2006).
In this study, we investigate how these recent changes in Australian climate have impacted upon the circulation of a subtropical east Australian coastal bay over the period 1990 to 2007. The study utilizes recent hydrographic observations from Hervey Bay (Fig. 1) and a coastal ocean general circulation model. Inter- and intra-annual local rainfall variability and drying trends are strongly linked to variability in the large-scale Pacific Ocean equatorial atmosphere and ocean circulation system. The coastal bay is shown to be dominated by an inverse circulation and recent changes in climate are associated with changes in the physical properties of the bay. Hypersalinity is a persistent feature and is more frequent in the last decade due to regional climate changes. This has implications for water quality and ecological response to inputs from the watershed and from the coastal ocean.

Corresponding author address: Ulf Gräwe, University of Oldenburg / ICBM, Carl-von-Ossietzky-Str. 9-11, 26111 Oldenburg/Germany; e-mail: graewe@icbm.de

	Summer	Fall	Winter	Spring	Annual
Precipitation	452	230	126	200	1008
Evaporation	644	455	326	555	1980
River discharge	72	66	25	11	174
				net loss	798

Table 1: *Climatological water balance (in mm/m²) of Hervey Bay (southern hemisphere seasons).*

2. MODELL DESCRIPTION

We employ the hydrodynamic part of the three dimensional primitive equation ocean model COHERENS (COupled Hydrodynamical Ecological model for REgioNal Shelf seas) (Luyten et al. 1999). Some basic features of the model can be summarised as follows: the model is based on a bottom following vertical sigma coordinate system with spherical coordinates in the horizontal. The hydrostatic assumption and the Boussinesq approximation are included in the horizontal momentum equations. The sea surface can move freely, therefore barotropic shallow water motions such as surface gravity waves are included. The simulation of vertical mixing is achieved through the 2.5 order Mellor-Yamada turbulence closure (Mellor et al. 1982). The horizontal turbulence is taken proportional to the product of lateral. grid spacing and the shear velocity (Smagorinsky 1963) Advection of momentum and scalar transport is implemented with the TVD (Total Variation Diminishing) scheme using the superbee limiting function (Roe 1985). These are standard configurations provided with COHERENS. For further details of numerical techniques employed see Luyten et al. (1999).

2.1 Boundary conditions

Because the simulations heavily rely on the proper calculations of air-sea fluxes, we modified the bulk parametrization in COHERENS by the COARE 3.0 algorithm (Coupled-Ocean Atmosphere Response Experiment, Fairall et al. 1996, 2003). The COARE 3.0 algorithm now includes various physical processes,

relating near-surface atmospheric and oceanographic variables and their relationship to the sea surface, to compute/estimate the transfer coefficients of latent heat C_L, sensible heat C_S, momentum C_D and moisture C_E. The total exchange coefficient for any relevant physical property *x*

$$C_x = \sqrt{c_x}\sqrt{c_D}$$

is decomposed into the wind depend part c_D and the bulk exchange coefficient of the tracer *x* under considerations. Here x can be *u*, *v* wind components, the potential temperature θ, the water vapour specific humidity *q* or some atmospheric trace species mixing ratio. These transfer coefficients have a dependence on surface stability prescribed by the Monin-Obukov similarity theory (MOST) (Monin 1953). Moreover the algorithm includes separate models for the ocean's cool skin and the diurnal warm layer, which are used to derive the true skin temperature. For details of the parametrization and also the iterative solution techniques employed see Fairall et al. 1996, 2003.

The long wave back radiation flux is computed using the formulation of Bignami et al. (1995):

$$H_{LW} = 0.98\ B\ T_S^4 - B\ T_{air}^4\ (0.65 + 0.0054\ Q_a)(1 + 0.176\ TCC^2)$$

where *S* is the Stefan-Boltzmann constant ($5.67*10^{-8}$ W $m^{-2}K^{-4}$, T_S and T_{air} are the water and air temperature in Kelvin and *TCC* the total cloud cover. This choice was motivated by the comparison of different back radiation parametrization by Josey et al. (2003). Here the formulation of Bignami et al. (1995) showed the best performance in subtropical regions.

Amplitudes and phases of the five major tidal constituents (M_2, S_2, N_2, K_1 and O_1) are prescribed at the open boundary. These five principal constituents explain nearly 80% of the total variance of the observations within Hervey Bay. Tidal elevations and phases are taken from the output of the global tide model/atlas FES2004 (Lyard et al. 2006) with assimilated altimeter data. Sea surface height (SSH), anomalies (SSHA) and also the sea surface gradient causing the EAC, are prescribed using TOPEX/Poseidon, JASON-1 altimeter data. The lateral open boundary conditions are implemented as radiative conditions according to Flather (1976). A quadratic bottom drag formula at the sea floor is used with a bottom roughness length of z_0 = 0.002 m. At the open-ocean boundaries we prescribe profiles of temperature and salinity that are derived from the global ocean model OCCAM (Saunders et al. 1999), which has a horizontal resolution of 1/4° and 66 vertical z-levels. Because the OCCAM model data set only provides five day averaged fields, the open ocean boundary conditions are therefore updated every fifth day.

2.2 Model design

The model domain is resolved using a coarser grid for the outer area and a finer grid for Hervey Bay (one way nesting). The outer domain (see Fig. 1) is a orthogonal grid of 90*140 points. The mesh size varies and increases from 2.5 km within Hervey Bay to 7 km near the boundaries of the model domain. The model bathymetry is extracted from a high resolution bathymetry which provides a horizontal resolution of 250 m. The vertical grid uses 18 sigma levels with a higher resolution towards the sea surface and the bottom boundary. The reason is to resolve accurately the upper mixed layer, but also to catch gravity currents at the sea floor. To minimize artificial geostrophic flows due to internal pressure errors caused by the use of sigma coordinates over bathymetry with steep gradients (Haney 1991, Beckman and Haidvogel 1993) the model bathymetry has been smoothed (Martinho et al. 2006). This reduced the artificial flows to less than 5 cm/s at the shelf edge. The maximum depth within the model domain is limited to 1100 m in order to increase the maximum allowable time step to 12 s and 360 s for the barotropic and baroclinic modes, respectively.

The inner domain (indicated by the red dashed line in Fig. 1) has a uniform grid spacing of 1.5 km and a size of 100*120 grid points. To be consistent with the outer domain the maximum depth was again limited to 1100 m, although, the vertical resolution remains the same. The time steps are then 7 s and 140 s for the barotropic and baroclinic modes, respectively.

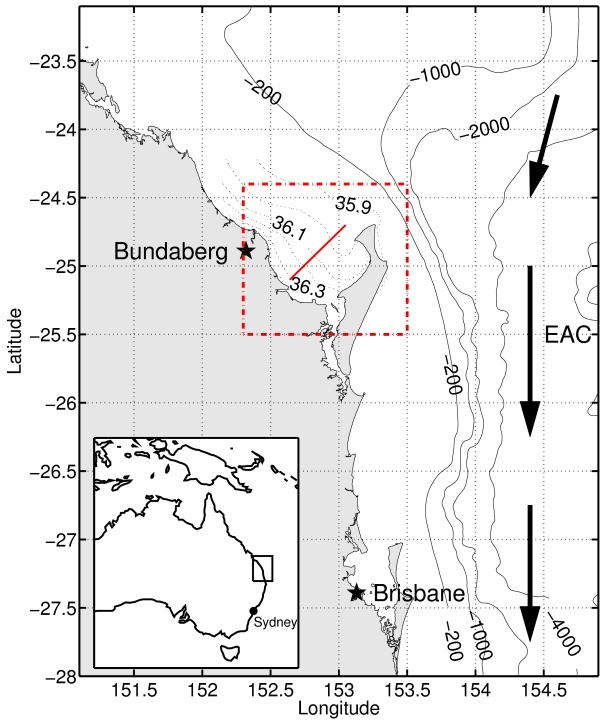

Figure 1: *Model domain and location of Hervey Bay. The red dashed box indicates the focus of the model data analysis. Salinities are analysed along the indicated transect. Also shown in the box is the mean salinity distribution averaged over the period 1990-2007. The East Australian Current (EAC) is schematically shown by the arrows. Insert: a map of Australia showing the location of the model domain along the east Australian coast.*

The vertical profiles of *U, V, T, S* and *SSH* of the outer model are interpolated onto the grid of the inner model domain.
To initialise the model a spin-up of two years (1988-1990) was used, starting from rest with climatological profiles for salinity and temperature. The numerical experiments analysed for this study cover the period 1990-2007.

3. DATA

Hydrographic observations, made during three one-week field trips into the bay in September 2004, August and December 2007 and Advanced Very High Resolution Radiometer (AVHRR) sea surface temperature (SST) data from 1999-2005 are utilized to validate the performance of the model. The September 2004 field trip provided the first indication that Hervey Bay is an inverse estuary. The sampling as well as an analysis of the hydrographic situation within the bay is presented by Ribbe (2006). Subsequent cruises confirmed that assessment. A detailed analysis of the data will be presented in a forthcoming presentation; here we focus on the validation of the modeled temperature and salinity structures in the bay and the use of the model to investigate the impact of recent climate changes on the inverse state of the bay. To force the model we are using three hourly observations of atmospheric variables (note that we use measured precipitation) of weather stations located along the east coast, which are interpolated onto the model domain. The river forcing is coming from daily observations of river discharge.

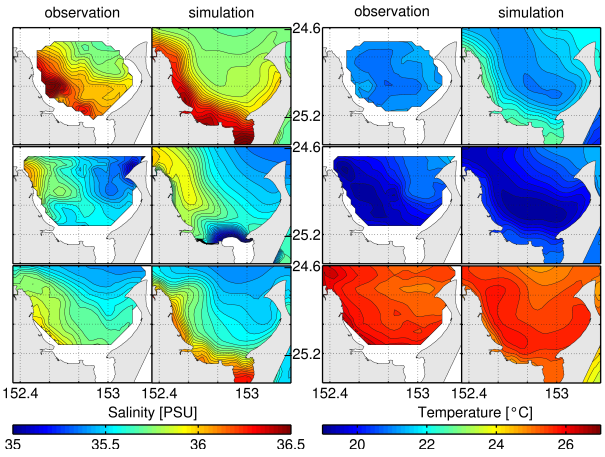

Figure 2: *Comparison of the depth-averaged salinity and temperature distributions during September 2004 (top), August 2007 (middle) and December 2007 (bottom).*

4. RESULTS

The simulated temperature and salinity distribution within Hervey Bay is consistent with the observations during all three field surveys (Fig. 2). The simulations reveal that the bay is in parts vertically well mixed throughout
most of the year. To quantify this we computed the bay averaged Richardson number. Most of the time this was less than the critical Richardson number of 1/4. Below this critical value the water column is controlled by vertical mixing. Only in spring we observed peak values of 0.5-0.9. Therefore, only the depth averaged quantities are considered here for model validation. The model reproduces the salinity gradient with salinity decreasing in all three field trips from the southwest coast towards the northern opening of the bay (Fig. 2). The comparison with the first survey shows that the salinity gradient is less sharp than indicated by the model. But in general the agreement of the model output and the measurements from each of the field trips is quite well. The model conforms with the observations that the coastal region is occupied by a zone of hypersalinity with salinities well above 36 PSU. The observed temperature distribution is reproduced by the model as well. There are some deviations for the September 2004 field trip. The model seems to overestimate the temperature in the near shore region, but both observations and simulated data show a similar pattern. The distribution of temperature is well matched by the model for both subsequent field trips. For further validation of the model performance, we compute the daily bay averaged SST for both model and AVHRR data. The two indices are highly correlated with a correlation coefficient exceeding 0.9 and a vanishing bias.
Encouraged by the good model performance in simulating the physics and hydrodynamics of Hervey Bay we applied the model to investigate the temporal evolution of the hypersalinity zone and the inverse nature of the bay in some more detail.

4.1 Inverse state

The hydrographic observations made during the three field surveys indicate that hypersalinity is likely to be a reoccurring climatological feature characterizing the bay. Climatological data for evaporation, precipitation and river runoff (see Tab. 1) show that evaporation with about 2 m/year by far exceeds the supply of freshwater into the bay from precipitation with about 1 m/year and very low river run-off (see Ribbe 2006 for details). The application of the ocean model allows us to investigate the distribution of salinity throughout time. In fact, the time averaged distribution of salinity in the bay (Fig. 1) confirms that the hypersalinity zone is a climatological feature for the period 1990-2007. The climatological mean value for the salinity gradient is in the order of about 0.5 PSU with salinities near the southwest of >36.5 PSU and near the open ocean in the northeast of about <35.9 PSU. The magnitude of this gradient corresponds to those observed during the three surveys. Figure 3 provides an indication of the temporal evolution of this gradient along the transect through the bay. Near coastal hypersalinity is revealed as a persistent feature throughout most of the time

(especially in the last half of the study period). The salinity gradient reverses only during significant rainfall events accompanied by somewhat delayed higher river discharges, i.e. the salinity near the coast is lower than towards the open ocean. This is for example the case during 1996 when the strongest reversal is observed.

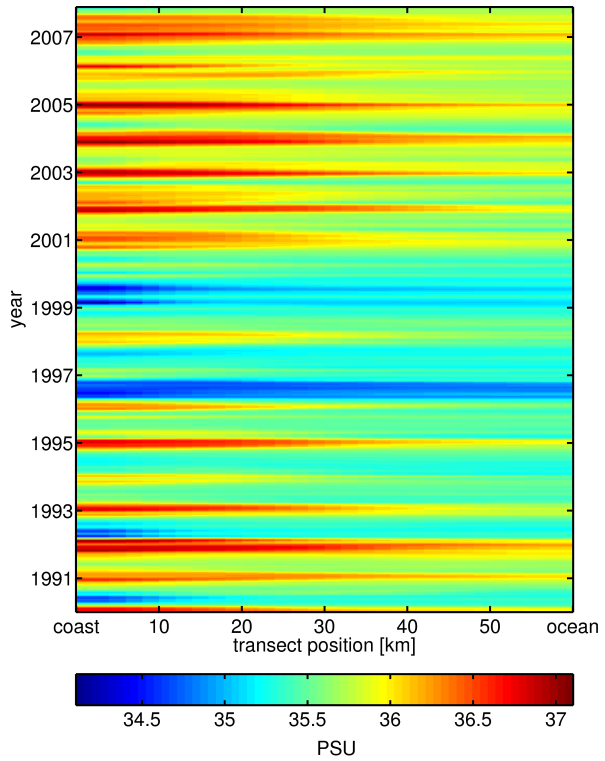

Figure 3: *Temporal evolution of the salinity along the transect (vertically averaged model results). In order to remove tidal modulations we used a 30 day running mean filter.*

Closer inspection of the time series (not shown here) for surface freshwater fluxes due to rainfall and river discharges reveal that during this year a particular wet winter prevents the maintenance of a hypersalinity zone from about April to November 1996. With the approach of summer and an increase of evaporation and no further significant freshwater discharges, the hypersalinity zone reforms (Fig. 3). It is interesting to note that during the last decade less frequent reversals of the salinity gradient occurred (Fig. 4). This is due to the reduced supply of freshwater to the region as a result of the continued east coast drying trend. The hypersalinity zone can lead to the formation of a dense water mass that is discharged from Hervey Bay and injected into the ocean to the north of the bay. To have a measure of this salt injection, we calculate the salinity import/export out of the bay by computing the transport by advection and diffusion through the open boundaries of the bay.

$$F_{Salinity}(t) = \int_A v(x,z,t) S(x,z,t) + K_H(x,z,t) \partial_y S(x,z,t)\, dA$$

The first term represents the flux by advection (meridional velocity times salinity) whereas the second term represents the diffusive fluxes. K_H is the turbulent scalar horizontal diffusivity. A rough estimate of the contribution to the integral can be given by estimating the average advective transport with 4 kgm/s, assuming a residual current of 0.1 m/s.

The model predicts a bay average turbulent diffusivity of 30 m^2/s. which is used to compute the diffusive transport. If one estimates the salinity gradient from the climatology (10^{-5} psu/m), this results in a diffusive transport of approx. $3*10^{-4}$ kgm/s. Therefore the advective transport is at least three orders of magnitude larger than the diffusive transport.

The mean transport/export of salinity is estimated to be approx. 4.0 tons/s (Fig. 4). If one uses the climatological values (Tab. 1), the net loss of 798 mm would result in an outflow of 3.7 ton/s, which is in good agreement with the numerical results. The model indicates that since 1990, the salinity flux has increased by about 25% (linear fit in Fig. 4). Shi et al. (2008a) pointed out, that the total annual mean rainfall in the region has significantly decreased over the last 50 years and the drying has accelerated in particular during the last 20 years. The trend, visible in our forcing time series, is estimated with a reduction of 15% in precipitation and 5% in river discharge. These trends would lead to a rise in salinity flux to 4.5 ton/s (21% increase during the last two decades) which is again comparable with the model prediction. The analysis of the simulation further showed that the annual mean heat content of the bay, solar heat flux and air temperature remain nearly constant over the whole simulation period. They are only responsible for the intra annual variability. The most important factor influencing the rising trend in the salinity gradient/salinity flux is therefore the positive difference between evaporation and precipitation/river discharge.

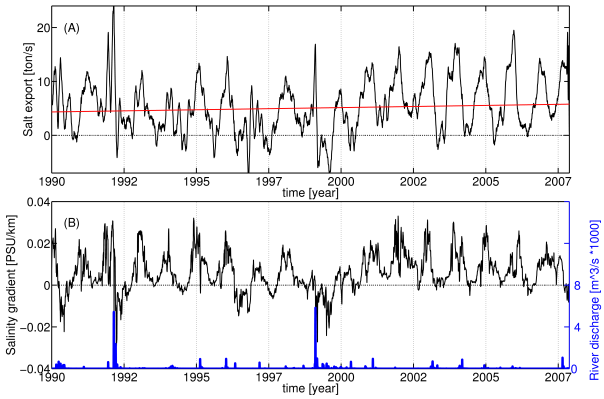

Figure 4: *(A) Salinity export [tons/s] and linear trend. To remove tidal modulations and also small scale atmospheric fluctuations we used a 30 day running mean filter. (B) salinity gradient [PSU/km] along the transect shown in Figure 1 from Hervey Bay. Also show is the influx of river freshwater that enters the bay (blue curve).*

5. CONCLUSIONS

Climatological data indicate that Hervey Bay exhibits features of an inverse estuary, due to the high evaporation rate of approximately 2 m/year, a low precipitation of less than 1 m/year and an on average

almost absent freshwater input from three rivers that drain into the bay. Here, we applied the ocean model COHERENS to compute the temperature and salinity distribution within the bay. A model validation and calibration is carried out using recent in-situ field and satellite AVHRR SST data. Observations and model results show that the bay is in parts vertically well mixed throughout the year. As in other inverse estuaries, the annual mean salinity increases towards the shore to form a nearly persistent salinity gradient. The region therefore acts as an effective source of salt accumulation and injection into the open ocean. The high evaporation is leading to a loss of freshwater and increases salinity within the bay. The average outflow of salt into the open ocean is computed as about 4.0 tons/ s. But the export of salt increased by 25% in the last two decades. This is due to an ongoing drying trend at the East Coast of Australia. The climate of subtropical eastern Australia has changed during the last few decades, and this study indicates that hypersalinity conditions are more persistent during the same period, salt discharges increase, and reversal of hypersalinity conditions are less frequent in the last decade due to the reduced supply of freshwater. Our study clearly demonstrates that recent climate trends impacted on physical marine conditions in subtropical regions of eastern Australia and are likely to do so in the future if current climate trends (drying) are to continue.

ACKNOWLEDGEMENTS

We would like to acknowledge financial support for this study provided by the Burnett Mary Regional Group, Australia, the Hanse Institute for Advanced Study, Delmenhorst, Germany and the Universitäts-Gesellschaft Oldenburg (UGO). We also gratefully acknowledge the Bureau of Meteorology, Australia, Geoscience Australia and CSIRO Marine and Atmospheric Research for providing various data for this study.

REFERENCES

Beer, T., Borgas, M., Bouma, W., Fraser, P., Holper, P., Torok, S., 2006: Atmosphere. Theme commentary prepared for the 2006 Australia State of the Environment Committee, Department of Environment and Heritage, Canberra

Brink, K. H. and Shearman, R. K., 2006: Bottom boundary layer flow and salt injection from the continental shelf to slope, J. Geophys. Res. Lett, 33, L13608.

Cai, W., Shi, G., Cowan, T., Bi. D., Ribbe, J. 2005. The response of the southern annual mode, the East Australian Current, and the southern mid-latitude ocean circulation to global warming, J. Geophys. Res. Lett, 32, L23706.

deCastro, M., Gomez-Gesteira, M., Alvarez, I., Prego, R. (2004): Negative estuarine circulation in the Ria of Pontevedra (NW Spain), Estuarine, Coastal and Shelf Science. 60, 301-312

Fairall, C.W., Bradley, E.F. ,Rogers, D.P. ,Edson, J.B., Young, G.S., 1996. Bulk parameterization of air-sea fluxes for tropical ocean-global atmosphere Coupled-Ocean Atmosphere Response Experiment, J. Geophys. Res., 101, 3747-3764.Fairall, C.W., Bradley, E.F., Hare, J.E., Grachev, A.A. , Edson, J.B. 2003, Bulk Parameterization of Air–Sea Fluxes: Updates and Verification for the COARE Algorithm. J of Climate 16, 571-591

Geernaert, G. L., Katsaros, K. B., and Richter, K. 1986: Variation of the drag coefficient and its dependence on sea state, J. Geophys. Res., 91, 7667-7679.

Largier, J.L., J.T. Hollibaugh and S.V. Smith, 1997. Seasonally hypersaline estuaries in Mediterranean-climate regions. Estuarine Coastal and Shelf Science 45, 789-797

Lavin, M.R., Godinez, V.M., Alvarez, L.G. 1998, Inverse-estuarine Features of the Upper Gulf of California, Estuarine, Coastal and Shelf Science. 47, 769-795

Luyten, P. J., Jones, J. E., Proctor, R., Tabor, A., Tett, P., and Wild-Allen, K. 1999: COHERENS - A coupled hydrodynamical-ecological model for regional and shelf seas: user documentation, MUMM Rep., Management Unit of the Mathematical Models of the North Sea.

Martinho, A.S., Batteen, M.L. 2006, On reducing the slope parameter in terrain-following numerical ocean models Ocean Modelling 13, 166–175

Mellor, G.L., Yamada, T. 1982, Development of a turbulence closure model for geophysical fluid problems. Rev Geophys Space Phys 20, 851-875

Murphy, B. F., Ribbe, J. 2004. Variability of southeast Queensland rainfall and its predictors, Int. Journal of Climatology, 24(6), 703-721.

Ribbe, J. 2006. A study into the export of saline water from Hervey Bay, Australia. Estuarine, Coastal and Shelf Science. 66, 550-558.

Ribbe, J., Wolff, J.-O., Staneva, J., Gräwe, U., 2008. Assessing Water Renewal Time Scales for Marine Environments from Three-Dimensional Modelling: A Case Study for Hervey Bay, Australia, Environmental Modelling and Software, In Press.

Seidel, D. J., Fu, Q., Randel, W. J., Reichler, T. J., 2008. Widening of the tropical belt in a changing climate. Nature Geoscience, 1, 21-24.

Shi, G., Cai, W., Cowan, T., Ribbe, J., Rotstayn, L., Dix, M., 2008a. Variability and trend of the northwest Western Australia Rainfall: observations and coupled climate modelling. Journal of Climate. In Press.

Shi, G., Ribbe, J., Cai, W., Cowan, T. 2008b. Interpretation of Australian summer and winter rainfall projections, J. Geophys. Res. Lett. 35, L02702.

Tomczak, M., and Godfrey, S., 2003. Regional Oceanography: an Introduction. 2nd edition.Daya Publishing House, Delhi, 390 pp.

Umlauf, L., Burchard, H., Second-order turbulence closure models for geophysical boundary layers. A review of recent work, Continental Shelf Research, Vol. 25, pp. 795-827.